Asociación Argentina de Mecánica Computacional

Mecánica Computacional Vol XXXI, págs. 3013-3025 (artículo completo)
Alberto Cardona, Paul H. Kohan, Ricardo D. Quinteros, Mario A. Storti (Eds.)
Salta, Argentina, 13-16 Noviembre 2012

BREAD CRUMB CLASSIFICATION USING FRACTAL AND MULTIFRACTAL FEATURES

Rodrigo Baravalle[a], Claudio Delrieux[b] and Juan Carlos Gómez[a]

[a]*Laboratorio de Sistemas Dinámicos y Procesamiento de Información, FCEIA, Universidad Nacional de Rosario, - CIFASIS - CONICET, Riobamba 250 bis, 2000, Rosario, Argentina, {baravalle,gomez}@cifasis-conicet.gov.ar, http://www.cifasis-conicet.gov.ar/index.php?grupo=4*

[b]*DIEC, Universidad Nacional del Sur - IIIE-CONICET, Avenida Colón 80 - Bahía Blanca(8000FTN) - Provincia de Buenos Aires - República Argentina, cad@uns.edu.ar, http://www.ingelec.uns.edu.ar/*

Keywords: Fractal, Multifractal, Classification, Bread crumb, Support Vector Machines

Abstract. Adequate image descriptors are fundamental in image classification and object recognition. Main requirements for image features are robustness and low dimensionality which would lead to low classification errors in a variety of situations and with a reasonable computational cost.

In this context, the identification of materials poses a significant challenge, since typical (geometric and/or differential) feature extraction methods are not robust enough. Texture features based on Fourier or wavelet transforms, on the other hand, do withstand geometric and illumination variations, but tend to require a high amount of descriptors to perform adequately.

Recently, the theory of fractal sets has shown to provide local image features that are both robust and low-dimensional. In this work we apply fractal and multifractal feature extraction techniques for bread crumb classification based on colour scans of slices of different bread types. Preliminary results show that fractal based classification is able to distinguish different bread crumbs with very high accuracy.

1 INTRODUCTION

Fractal and multifractal analysis of images have proved to capture useful properties of the underlying material being represented. Characterisation of images using these features have been successfully applied in different areas, such as medicine (Andjelkovic et al. (2008); Yu and Qi (2011)) and texture classification (Wendt et al. (2009)). Through several procedures, it is possible to obtain different Fractal Dimensions (FD), each of them capturing a different property of the material (*e.g.*, void image fraction, rugosity).

For each material, the results obtained in the classification process are useful in quality measurements of real samples and also in the validation of synthetic representations of them. In other words, the classification is useful to determine if a given image presents the observed features in that material, allowing to associate quality measure parameters to the material. In Fan and Zhang (2006), a quality bread crumb test based on Gabor filters was performed in that paper, obtaining good results. Nevertheless, a small database was used (30 images). In Gonzales-Barron and Butler (2008) several fractal features were obtained for one type of bread, showing that a vector comprising them would be capable of obtaining key features of its crumb texture.

In this work we propose the application of fractal and multifractal descriptors for the classification of different bread types and for the discrimination between bread and non-bread images. The proposed method is compared to a classifier that uses only mean colour information. The results of this feature extraction procedure show that the classifier is robust and presents good discrimination properties to distinguish between bread and non bread images. In section 2 we briefly introduce the theory underlying fractal sets. In section 3 we describe the materials and methods employed in the classification. In section 4 we show the results obtained in the classification and we perform a robustness analysis of the method. In section 5 we summarise the conclusions, and we pose some possible future works.

2 FEATURES

2.1 Box dimension

Box FD is a simplification of the Hausdorff (originally Minkowski - Bouligand) dimension for non strictly self-similar objects (Peitgen et al. (2004)). Given a binarised image, it is subdivided in a grid of size $M \times M$ where the side of each box formed is ϵ. If N_ϵ represents the amount of boxes that contains at least one pixel in the binarisation of the set for that ϵ, then the box dimension D_b is defined as

$$D_b \triangleq \lim_{\epsilon \to 0} \frac{\log(N_\epsilon)}{\log(1/\epsilon)}. \tag{1}$$

The algorithm computes a binarised image from the original one and then selects different values of ϵ in it, making a count of the boxes that contains pixels in each case (to avoid numerical instabilities, a mean of cases is computed, establishing different positions in the grid over the image). Finally, a linear regression adjustment is made with the obtained data, in the $\log - \log$ space, and the slope of the straight line is by definition the box dimension of the image. In Fig. 1 an image of the bread type *salvado* is shown with its corresponding box dimension computation.

2.2 Morphological fractal

This FD is computed through dilation and erosion operations, using a structuring element (SE). The transformed image is a function of the distribution of that particular SE in the original image. In Gonzales-Barron and Butler (2008), the SE selected was a rhombus Y with scales

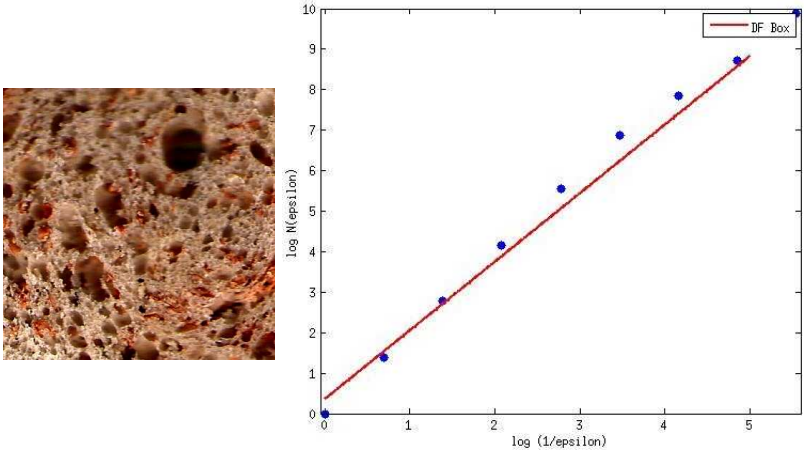

Figure 1: An image and its computed box dimension

that varies from $\epsilon = 1$ to $\epsilon = 7$ (and the areas of the SE between 5 and 113 pixels). The surface area $S(X, Y, \epsilon)$ can be calculated, for each ϵ as

$$S(X, Y, \epsilon) = \frac{\sum_{x,y \in M}(f_\epsilon^u(x, y) - f_\epsilon^l(x, y))}{2\epsilon}, \tag{2}$$

where $f_\epsilon^u(x, y)$ is the ϵ-th dilation and $f_\epsilon^l(x, y)$ is the ϵ-th erosion of the original image. The morphological FD M_d is estimated from the slope of a linear regression adjustment of the data in $S(X, Y, \epsilon)$ and ϵ in the $\log - \log$ space as

$$M_d = 2 + m, \tag{3}$$

where m is the slope of the straight line fit.

2.3 Multifractal analysis

Some elements in nature show fractal features or auto similarity. The fractal dimension is an exponent which relates the statistical auto similarity of the object at different scales. On the one hand, deterministic fractals are characterized by the same FD at all scales. They are called *monofractals* (for instance, Koch Curve, Sierpinsky triangle). On the other hand, *multifractals* (Mandelbrot (1989)) are characterized by a set of FDs depending on the scale. It is assumed that these structures are composed by different fractals coexisting simultaneously. In a previous work (Baravalle et al. (2012)), it has been shown, using the Box Dimension and the Korcak Dimension (Imre et al. (2011)), that the bread crumb texture presents multifractal features. As a consequence, fractal and multifractal features are considered in the present paper.

2.3.1 Hölder exponent

Informally, the way to proceed with multifractal analysis is to examine, in the limit, the local behaviour of a measure μ at each point of the set under study. This means, to find the Hölder exponent α in that point. The *multifractal spectrum* $f(\alpha)$ is obtained applying this procedure to the entire set, in this case, an image.

Let E be an structure divided in disjoint substructures E_i of size ϵ in such a way that

$$\bigcup_i E_i = E. \tag{4}$$

Each substructure E_i is characterized by a measure $\mu(E_i)$. From the point of view of multifractal analysis, it is useful to define this value as a function of ϵ, *i.e.*

$$\alpha_i = \frac{ln(\mu(E_i))}{ln(\epsilon)}, \tag{5}$$

and to take the limit when ϵ tends to 0. The limit represents the value of the Hölder exponent at a point in the structure, that is

$$\alpha = \lim_{\epsilon \to 0} \alpha_i. \tag{6}$$

The exponent characterizes the local regularity of the structure at a point. To obtain a global characterization of its regularity it is necessary to obtain the distribution of α in E. For this, a counting N_ϵ must be done for each α_i, related to the value of ϵ, *i.e.*

$$f_\epsilon(\alpha_i) = -\frac{ln(N_\epsilon(\alpha_i))}{ln(\epsilon)}. \tag{7}$$

When ϵ tends to 0, the limiting value is the FD of the structure E characterized by α, the Hausdorff dimension of the α distribution, also known as the *multifractal spectrum* $f(\alpha)$ (Silvetti and Delrieux (2010)), *i.e.*

$$f(\alpha) = \lim_{\epsilon \to 0} f_\epsilon(\alpha). \tag{8}$$

2.3.2 Procedure

To obtain the Hölder exponent at a given pixel, a linear regression fitting is needed using the values ($log(\epsilon)$,$log(\mu(E_i))$, for $\epsilon = 2i + 1, i \geq 0$, where E_i are boxes of side ϵ centred at the pixel. The slope of the straight line fit is the desired Hölder exponent.

From the α values a new image is generated in grey scale (α image), with the same dimensions of the original, where the value at each pixel is a mapping from the exponent to that scale. Since it is possible to obtain $M \times M$ values per image (where $M \times M$ is the dimension in pixels of the image), it is necessary to define a number C of classes (the number could be a parameter), each of which establishes α range values, and then to calculate the spectrum only for those values.

Let α_{min} and α_{max} be the minimum and maximum values of α computed in the image. C values are defined $\alpha_c = \alpha_{min} + (c-1)(\alpha_{max} - \alpha_{min})/C$, where $c = 1, 2, \ldots, C$. Then, $\alpha \in \alpha_c$ if $\alpha_c \leq \alpha < \alpha_{c+1}$. If $\alpha = \alpha_{max}$, then $\alpha \in \alpha_C$. Finally, a linear regression fitting is obtained for the values $N_\epsilon(\alpha)$ and ϵ in the $\log - \log$ space. The value of the slope is the FD $f(\alpha_c)$ and must be calculated for $c = 1, 2, \ldots, C$. In this way C $f(\alpha)$ values are obtained, representing C FDs (C α_c associated values are also obtained). In this work, all these values are used as features in the classification (so $2 \times C$ features are obtained from the multifractal analysis). In Fig. 2 an image of *lacteal* bread type and its multifractal spectrum are shown (in this case, $C = 20$).

3 MATERIALS AND METHODOLOGY

3.1 Image acquisition

Fifty images of four different bread types (*lactal*, *baguette*, *salvado* and *sandwich*), counting two hundred images, were obtained using an electric slicer. The images were digitalised using

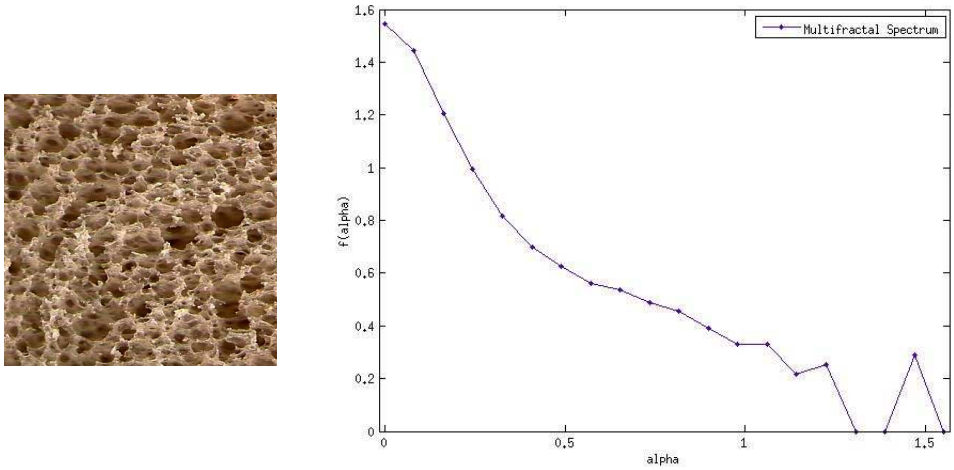

Figure 2: Bread image and its corresponding multifractal spectrum (20 FDs)

an HP PSC 1210 scanner and they were saved in TIFF format. Images showed a resolution of 380×380 pixels (the maximum possible area for the four bread types) and 350 dpi (1 pixel $=$ $0.00527mm^2$). Then the images were converted to grey scale (8 bits). In addition, 20 images of each bread type were acquired with a digital camera, using the same spatial resolution, counting 80 images. The illumination conditions of these images were different from that of the scanner in order to test for the robustness of the method. In Fig. 5 four examples of bread images from the camera are shown. We also employed one hundred randomly selected images from the CalTech101 (Fei-Fei et al. (2004)) dataset in order to test the method's performance with non-bread images. In Fig. 4 four examples of non-bread images from this dataset are shown.

For the FDs that uses a binarisation of the original image, the algorithm presented in White and Rohrer (1983) was used. This algorithm applies a local thresholding schema, which showed better results than using a global thresholding schema. Particularly, the algorithm presented in Huang and Wang (1995) and used in Gonzales-Barron and Butler (2008), showed poor results when the illumination conditions vary. Also an adjustment needs to be made since the centre of air bubbles with large areas appeared as black pixels, instead of white (and since those areas are characterized as dark regions in the original image), a global grey threshold is obtained using Otsu's algorithm (Otsu (1979)). Then this threshold is multiplied by a scalar which is a user defined parameter, defining as white the pixels with grey values below the threshold. It was found that defining the scalar as 0.8 showed acceptable results. So the combination of local and global thresholding makes it a hybrid algorithm. In Fig. 3 an image of each bread type used in this work (top row) and its resulting binarisation using the proposed algorithm (bottom row) is shown.

3.2 Feature vectors

Following the ideas presented in Gonzales-Barron and Butler (2008), the mentioned fractal and multifractal features were obtained for each image (using 20 Hölder exponents). For each image, a 42-dimensional feature vector was computed. The code of the algorithms for the computation of the Box dimension, the Morphological fractal dimension and the multifractal spectrum were written and run in Matlab. In order to make a comparison, a 3-dimensional feature vector, with RGB colour features was also computed (R mean, G mean, B mean).

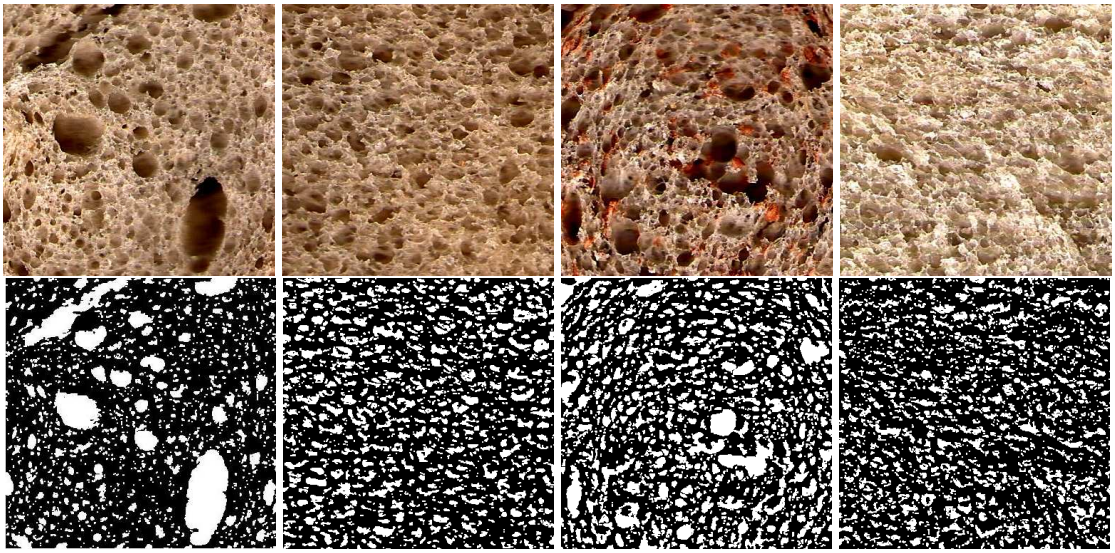

Figure 3: Digitalised images of *baguette*, *lactal*, *salvado* and *sandwich* bread types with its binarisations

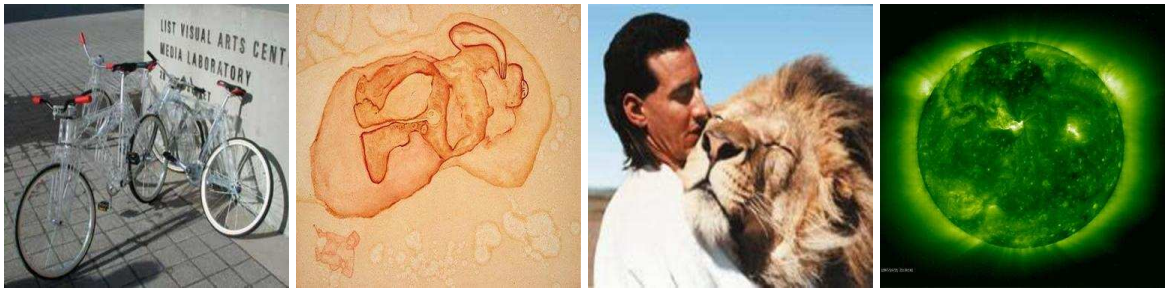

Figure 4: Images from the dataset CalTech101

Self-organizing maps (SOM) (Kohonen et al. (2001)) of the vectorized images are useful to visualize these different representation of bread images into a lower dimensional view, in order to understand them better. A SOM maps high dimensional data into a (typically) two-dimensional representation, using neighbourhood information. Topological information of the original data is preserved.

Unsupervised SOM of the fractal and non fractal representations of scanned images are shown in Fig. 6a and Fig. 6b respectively. The fractal features SOM seems to show easily separable classes while the RGB features SOM appears to be more overlapped. It seems that a classifier could potentially obtain better classification results using the fractal features.

4 RESULTS

4.1 Classification

Support Vector Machines (SVM) (Boser et al. (1992)) were used to perform the classification, using the *libsvm* (Chang and Lin (2011)) implementation. The method of *k-fold cross validation* was employed in order to validate the results with $k = 4$, *i.e.*, 75% of samples are used as training and 25% as testing (then switching the training and testing samples). Table 1 shows classification results for both classifiers and also for the combined features classifier (*i.e.*, employing feature vectors comprising fractal and colour features), using 50 scanned images of

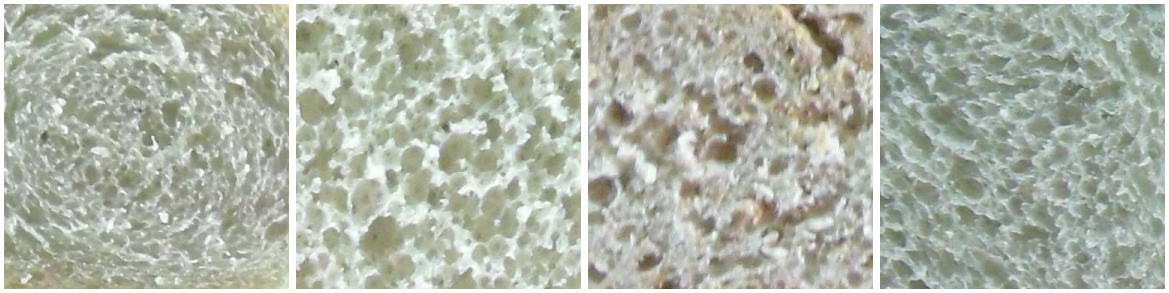

Figure 5: Digitalised images from a digital camera

each type (*i.e.* 250 images, including 50 of non bread images, scaled to the size of bread images). It can be seen that the use of non-fractal features in the images gives comparable results to that of using fractal features.

Features	Fractals	non Fractals	combined
Accuracy	93.2%	88.0%	**94.4%**

Table 1: Results obtained in classification

In addition, bread images of a different bread type, from the database employed in Gonzales-Barron and Butler (2008), were facilitated by Dra. Gonzales Barron. They were digitalised both using a scanner and using a digital camera. From this database, we added one class to the classification in order to obtain 300 images, employing 50 digitalised images from the scanner, with the same spatial resolution of the other bread images. The images were received in grey scale, *i.e.*, only the fractal features could be considered. The performance of the classifier for the fractal features was maintained, with an accuracy of 94.3%. In Fig. 7, two images of this bread type, digitalised using a scanner (left) and using a digital camera (right) are shown.

4.2 Robustness tests

A robust bread crumb classifier could be used to make the classification process independent of the image capturing condition. In order to test for the robustness of the method, two tests were performed. The first test shows the accuracy of the classifiers when the training and the testing samples are images taken from a set formed with images captured in different conditions. The second test shows the performance of the classifiers when there is a capturing condition mismatch between training and testing samples.

4.2.1 Classification with different capturing methods

Table 2 shows classification results for the three classifiers, training a classifier with 20 scanned images and 20 camera images of each bread type (*i.e.* 200 images, including 40 samples of non bread images).

Features	Fractals	non Fractals	combined
Accuracy	86.5%	72%	**89.5%**

Table 2: Results obtained in classification using training samples from the camera and from the scanner

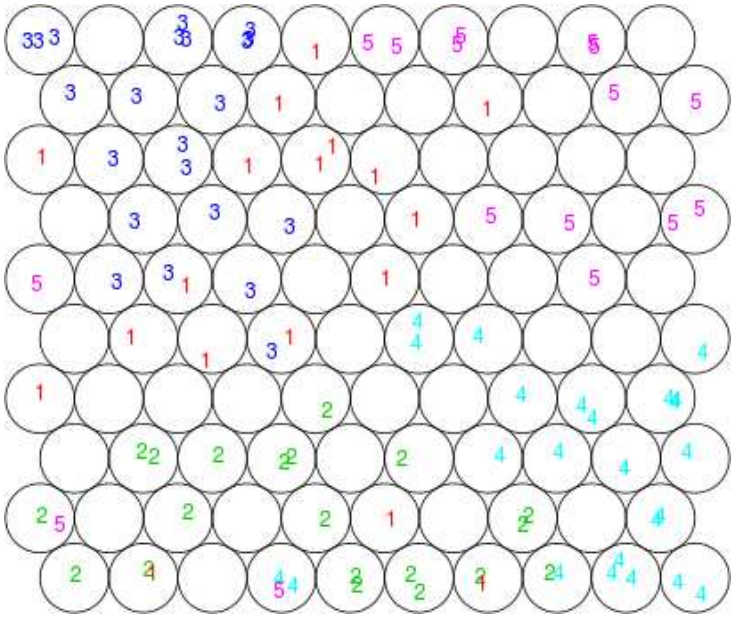

(a) Fractal features SOM

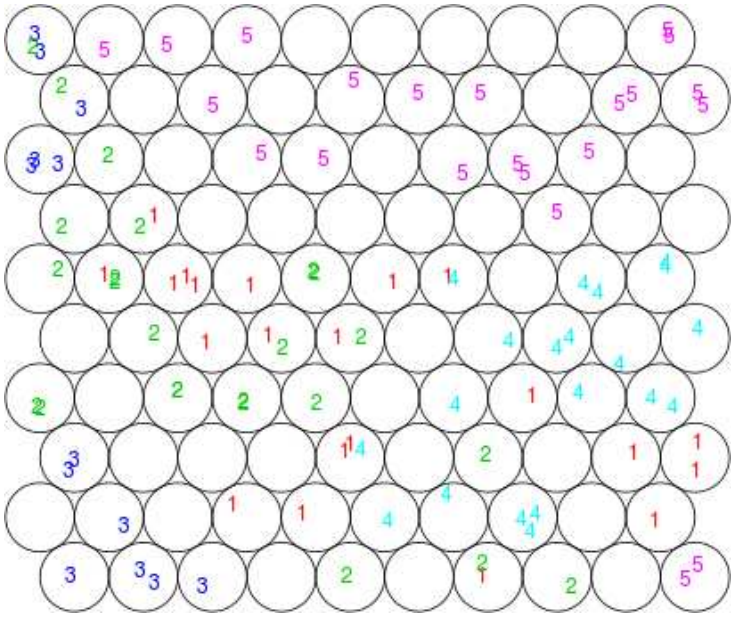

(b) SOM using RGB features

Figure 6: SOM of the scanned bread images (classes $1 - 4$) and the non bread images (class 5)

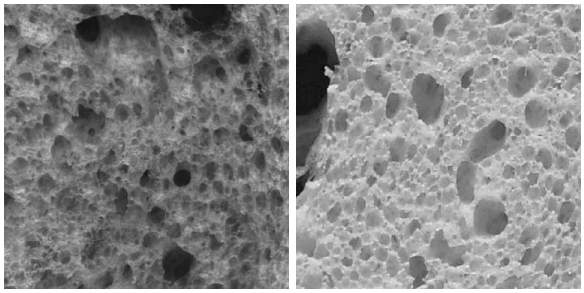

Figure 7: Images from Gonzales-Barron and Butler (2008) digitalised using a scanner (left) and using a digital camera (right)

Results show that the accuracy decreases approximately 7% for the fractal features. In addition, the accuracy of the non fractal features decreases more than the fractal ones. The combined classifier shows the best performance of the three classifiers, and a similar accuracy decrease to the fractal features. In addition, training and testing labels were relabelled to *bread-non bread* in order to obtain *Receiver Operating Characteristic* (ROC) curves for the classifiers. In Figs. 8a, 8b, 8c the ROC curves for the three classifiers show that the fractal features have the highest *Area Under Curve* (AUC), *i.e.*, it shows the best performance in the discrimination of bread images from non bread ones.

Images facilitated by Dra. Gonzales Barron were also included in the classifier, *i.e.*, 20 images from the scanner and 20 images from the camera (counting 240 images for the classification). The obtained accuracy for the fractal features (87.0833%) shows that the performance is maintained.

4.2.2 Classification when training with only one capturing method

The second test consists of 20 scanned images from each class, and 20 from the CalTech101 dataset, which were used for training, and all the images from the digital camera (20 per class), and 20 non bread images were used for testing (100 images for training and 100 images for testing). In Table 3 accuracy results of the three classifiers are shown. As expected, due to the mismatch between the training and the testing sets, the results show poor performance of the classifiers. In Tables 4, 5 and 6, the confusion matrix of the data using the three classifiers is shown. It can be seen that the RGB classifier assigns all the data to the non bread class, while the fractal and the combined features classifiers are able to discriminate between bread and non bread images, making them good discriminators of non bread images.

Features	Fractals	non Fractals	combined
Accuracy	**50**$\%$	20%	45%

Table 3: Results obtained when training with a capturing condition and testing with a different one

4.3 Deceiving the classifiers

It is possible to mislead the classifiers with false images. Fig. 9a shows an image obtained from Wikimedia[1] that is classified as bread by its RGB features. Fig. 9b shows an image gener-

[1] https://secure.wikimedia.org/wikipedia/commons/wiki/Sand

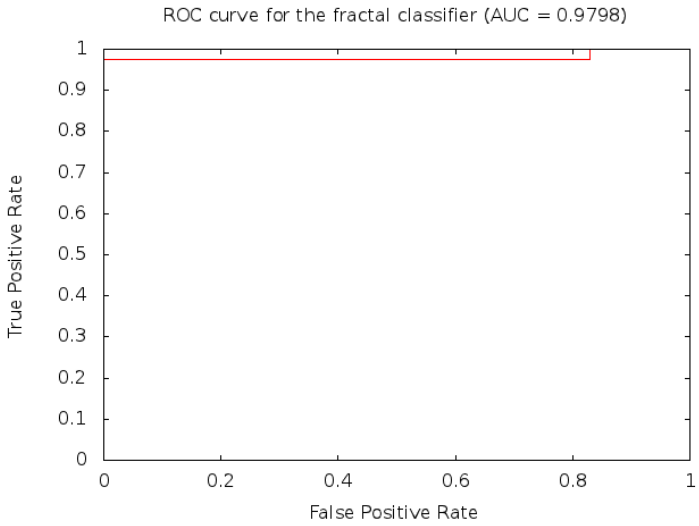

(a) ROC using fractal features

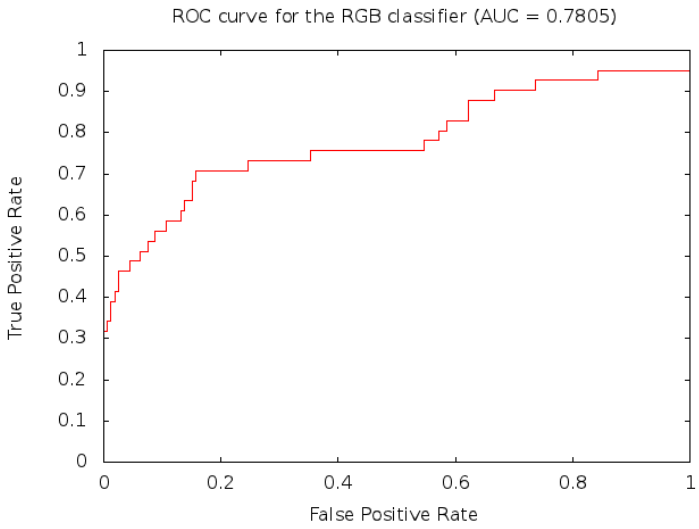

(b) ROC using RGB features

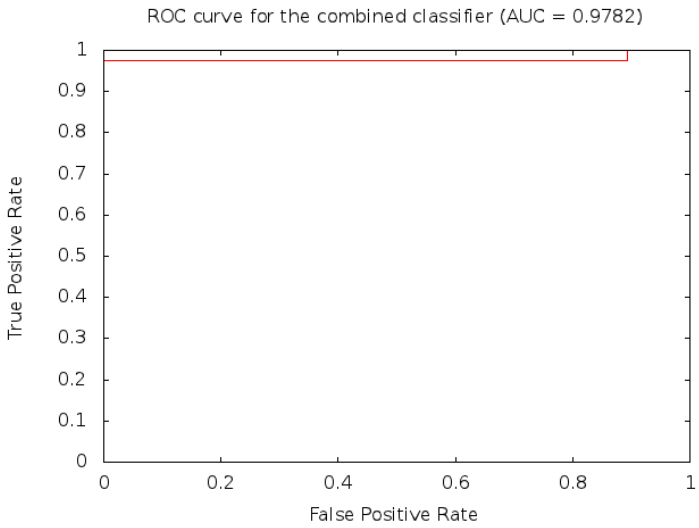

(c) ROC using both features

Figure 8: ROC curves for the binary classifiers (bread - non bread)

Classes	*baguette*	*lactal*	*salvado*	*sandwich*	non bread
baguette	0	11	0	9	0
lactal	0	19	0	1	0
salvado	1	11	0	8	0
sandwich	0	9	0	11	0
non bread	0	0	0	0	20

Table 4: Confusion Matrix for the fractal features

Classes	*baguette*	*lactal*	*salvado*	*sandwich*	non bread
baguette	0	0	0	0	20
lactal	0	0	0	0	20
salvado	0	0	0	0	20
sandwich	0	0	0	0	20
non bread	0	0	0	0	20

Table 5: Confusion Matrix for the RGB features

Classes	*baguette*	*lactal*	*salvado*	*sandwich*	non bread
baguette	0	6	0	14	0
lactal	0	7	0	13	0
salvado	1	6	0	13	0
sandwich	0	1	0	19	0
non bread	1	0	0	0	19

Table 6: Confusion Matrix for the combined features

ated by a particle system (Baravalle et al. (2011)) which is classified as bread by its fractal and multifractal features. It is easy to deceive the RGB classifier, using images with similar colour features as bread, but it is not clear how to do that with fractal features. We conclude that the fractal classifier is more suitable for the discrimination of these false images.

5 CONCLUSIONS AND FUTURE WORK

The use of fractal and multifractal features in bread crumb texture classification showed good performance. The multifractal spectrum demonstrated to be accurate enough to perform a classification of different bread types and also to discriminate non bread from bread images. The use of non-fractal features such as colour, also showed comparable results, but it fails to detect non bread images, and it is easy to deceive it with false images. The combination of both classifiers showed similar results to those obtained using the fractal features, so the use of the latter alone is preferred. The three classifiers showed to be sensitive to illumination changes, making them still non robust. Preliminary tests on our particle system (Baravalle et al. (2011)) show that it could deceive the fractal classifier, so further analysis is required in order to find the parameters that produce textures with similar fractal and multifractal features to those of real breads.

The results found can be applied to validate synthetic samples, *i.e.*, the latter should have similar features to the bread type that is trying to simulate. The features obtained will be used to determine particle system parameters (*e.g.*, lifetime of particles, colour). These results can

(a) RGB features (b) Mutilfractal features

Figure 9: Non bread images classified as bread by the evaluated classifiers

be extended to be used as quality parameters for these products. The robustness of the method needs to be enhanced. Other FDs will be studied in order to accomplish this goal. Also, the code of the multifractal spectrum algorithm needs to be optimized in order to obtain a faster algorithm for bread classification. It will be useful to apply a Principal Component Analysis in order to identify the key variables in the feature vectors.

6 ACKNOWLEDGEMENTS

We would like to thank Gustavo Grieco and Pablo Speciale for technical discussions and for their support in the development of the present work. We would also like to thank Dra. Ursula Gonzales-Barron for the received images.

REFERENCES

Andjelkovic J., Zivic N., Reljin B., Celebic V., and Salom I. Classifications of digital medical images with multifractal analysis. In *Proceedings of the 8th conference on Signal, Speech and image processing*, SSIP'08, pages 88–92. World Scientific and Engineering Academy and Society (WSEAS), Stevens Point, Wisconsin, USA, 2008.

Baravalle R., Delrieux C., and Gómez J.C. Síntesis de texturas utilizando sistemas de partículas. In *Actas de la Tercera Escuela y Workshop Argentino en Ciencias de las Imágenes (ECImag)*. 2011.

Baravalle R., Delrieux C., and Gómez J.C. Síntesis procedimental de materiales: resultados en el modelado de pan y materiales cocidos. In *Actas del XIV Workshop de Investigadores en Ciencias de la Computación (WICC)*, pages 21 – 26. 2012.

Boser B.E., Guyon I.M., and Vapnik V.N. A training algorithm for optimal margin classifiers. In *Proceedings of the fifth annual workshop on Computational learning theory*, COLT '92, pages 144–152. ACM, New York, NY, USA, 1992.

Chang C.C. and Lin C.J. LIBSVM: A library for support vector machines. *ACM Transactions on Intelligent Systems and Technology*, 2:27:1–27:27, 2011.

Fan Y. and Zhang H. Application of gabor filter and multi-class svm in baking bread quality classification. In *Mechatronics and Automation, Proceedings of the 2006 IEEE International Conference on*, pages 1498 –1502. 2006.

Fei-Fei L., Fergus R., and Perona P. Learning generative visual models from few training

examples an incremental bayesian approach tested on 101 object categories. In *Proceedings of the Workshop on Generative-Model Based Vision*. Washington, DC, 2004.

Gonzales-Barron U. and Butler F. Fractal texture analysis of bread crumb digital images. *European Food Research and Technology*, 226:721–729, 2008.

Huang L.K. and Wang M.J.J. Image thresholding by minimizing the measures of fuzziness. *Pattern Recognition*, 28(1):41 – 51, 1995.

Imre A.R., Cseh D., Neteler M., and Rocchini D. Korcak dimension as a novel indicator of landscape fragmentation and re-forestation. *Ecological Indicators*, 11(5):1134–1138, 2011.

Kohonen T., Schroeder M.R., and Huang T.S., editors. *Self-Organizing Maps*. Springer-Verlag New York, Inc., Secaucus, NJ, USA, 3rd edition, 2001.

Mandelbrot B.B. Multifractal measures, especially for the geophysicist. *Pure and Applied Geophysics*, 131:5–42, 1989.

Otsu N. A Threshold Selection Method from Gray-level Histograms. *IEEE Transactions on Systems, Man and Cybernetics*, 9(1):62–66, 1979.

Peitgen H.O., Jürgens H., and Saupe D. Chaos and fractals: new frontiers of science. 2004.

Silvetti A. and Delrieux C. Multifractal analysis of medical images. In *Actas de la trigésimo novena Jornada Argentina de Informática e Investigación Operativa (JAIIO)*, pages 1575 – 1581. 2010.

Wendt H., Abry P., Jaffard S., Ji H., and Shen Z. Wavelet leader multifractal analysis for texture classification. In *16th IEEE International Conference Image Processing (ICIP)*, pages 3829 –3832. 2009.

White J.M. and Rohrer G.D. Image thresholding for optical character recognition and other applications requiring character image extraction. *IBM J. Res. Dev.*, 27(4):400–411, 1983.

Yu L. and Qi D. Holder exponent and multifractal spectrum analysis in the pathological changes recognition of medical ct image. In *Control and Decision Conference (CCDC), 2011 Chinese*, pages 2040 –2045. 2011.